Biosensors and Bioelectronics 85 (2016) 171–177

Contents lists available at ScienceDirect

Biosensors and Bioelectronics

journal homepage: www.elsevier.com/locate/bios

Cratylia mollis lectin nanoelectrode for differential diagnostic of prostate cancer and benign prostatic hyperplasia based on label-free detection

Priscila M.S. Silva [a,b], Amanda L.R. Lima [b], Bárbara V.M. Silva [a], Luana C.B.B. Coelho [b], Rosa F. Dutra [a,*], Maria T.S. Correia [b]

[a] Biomedical Engineering Laboratory, Federal University of Pernambuco, Recife, Brazil
[b] Protein Biochemistry Laboratory, Federal University of Pernambuco, Recife, Brazil

ARTICLE INFO

Article history:
Received 2 January 2016
Received in revised form
1 May 2016
Accepted 2 May 2016
Available online 3 May 2016

Keywords:
Cratylia mollis lectin
Electrochemical biosensor
Carbon nanotube
Poly-L-lysine
Gleason score
Prostate cancer

ABSTRACT

The research for new biomarkers of cancer has studied the role of fetuin glycoprotein on the metastatic disease diagnosis. *Cratylia mollis* is a lectin with high finity to fetuin, and used here to differentiate prostate cancer and benign prostatic hyperplasia. A label-free electrochemical nanosensor based on assembled carboxylated carbon nanotubes (COOH-CNTs) and poly-L-lysine (PLL) film was developed and applied to serum samples of prostate cancer positive for Gleason score. The electrode analytical response to fetuin in PBS samples, obtained by square wave voltammetry, exhibited a linear range from 0.5 to 25 $\mu g\,mL^{-1}$, with a high correlation coefficient ($r=0.994$, $p<0.001$) and low limit of detection ($0.017\ \mu g\,mL^{-1}$). The lectin nanoelectrode showed a good repeatability (1.24% RSD) and reproducibility (4.24% RSD). A pool of serum samples from prostate cancer patients with known the Gleason score were tested showing a significant statistically correlation. Thus, the lectin nanoelectrode was able to distinguish the degree of staging prostate cancer, providing the diagnostic differentiation of benign and malign hyperplasia. To the best of our knowledge, it is the first biosensor for this application using a lectin.

1. Introduction

Prostate cancer (PCa) is the second most common cause of cancer death in men, after lung cancer, in worldwide (Siegel et al., 2014). The Prostate-specific antigen (PSA) is the gold-standard marker for PCa diagnostic used in clinical routine (Heidenreich et al., 2014). However, the PCa screening based on PSA levels has been associated to high false-positive rates (Moyer, 2012). The early staging of PCa facilitates the appropriate treatment, mainly for patients with high Gleason score that are more likely to progress for metastasis (Pierorazio et al., 2013). Despite extensive efforts, the lack of reliable methods for prediction of progression beyond early-stage disease and paucity of treatment options for patients with bone metastasis results in many patients with localized disease subjected to aggressive treatment with sequelae including incontinence and impotence (Schover et al., 2002). Thus, identification of biomarkers to improve the accuracy of clinical assessment of PCa constitutes a great challenge.

The fetuin glycoprotein has been studied as a new potential biomarker for pancreatic and liver cancers and tested in metastasis of tumor cells (Sakwe et al., 2010; Yi et al., 2009). Fetuin acts as an extracellular adhesive protein that conjointly with annexins induces cell adhesion and growth (Drake et al., 2006; Rho et al., 2009). Due to great importance as biomarker, different fetuin assays have emerged using auto antibodies against fetuin, like enzyme-linked immunosorbent assay-based in vitro diagnostic procedure (Vashist et al., 2015a), sandwich immunoassay using agarose-3-aminopropyltriethoxysilane modified microtiter plate (Vashist et al., 2015b) and surface plasmon resonance biosensor (Vashist et al., 2012', 2014). Fetuin is a glycoprotein, then the great interaction with specific lectins has been strategically explored by some authors. Bertok et al., (2013) developed a biosensor using the *Sambucus nigra* lectin for the determination of sialylated fetuin glycoproteins and asialofetuin in PBS; Oliveira et al., (2011) demonstrated that *Cratylia mollis lectin* (*Cramoll*) strongly interacted with fetuin using an impedimetric biosensor.

To improve accuracy of PCa diagnostic on metastatic phase, Mintz et al. (2015) published the first report associating fetuin as a potential marker for prostate cancer and demonstrated its prognostic utility as indicator for metastasis and aggressiveness of tumor. Herein, *Cramoll* was immobilized on a nanostructured electrode to successfully distinguish positive prostate cancer and

* Corresponding author.
E-mail address: rosa.dutra@ufpe.br (R.F. Dutra).

http://dx.doi.org/10.1016/j.bios.2016.05.004
0956-5663/

benign prostate hyperplasia (BPH) patients. This found correlated with Gleason score showing a significant concordance. To our knowledge, this is the first report of a biosensor using *Cratylia mollis* lectin to differentiate PCa and benign hyperplasia.

Electrochemical approaches like biosensors are of particular interest as transducers due to their ease mass production, portable and low cost (Bertok et al., 2013). They also provide a friendly instrumentation, and a great compatibility with portable systems suitable for point-of-care testing (Ahmed et al., 2016). Some electrochemical biosensors based on impedance spectroscopy using lectins as marker for fetuin detection have been developed (La Belle et al., 2007; Oliveira et al., 2011; Bertok et al., 2013). Although, these biosensors had advantages of non-requirement of a tracer or label, allowing a rapid detection, they require more careful in measurements due to frequent noises and misinterpretations when compared to recent methods of electrochemical label-free immunosensors, such as square-wave voltammetry (SWV) technique. This method is based on staircase of potential pulse superimposed on a staircase potential signal with the latter centred between a cathodic and anodic pulse of the same amplitude, allowing to discriminate the capacitive current with high sensitivity (Liu et al., 2010).

The use of nanomaterials for biosensors based in film, particularly carbon nanotubes (CNTs) have attracted considerable attention due to provide a high surface-volume ratio, faster electron transfer and label-free responses (Gomes-Filho et al., 2013). Synergic effect between CNTs and polymers was explored to make the nanostructured films more stable with higher electrocatalytic activity (Silva et al., 2014). Additionally, CNTs are easily functionalized by chemical or thermal reactions (Ma et al., 2010), promoting irreversible processes of biomolecules immobilization on electrode surface (Freitas et al., 2014). Herein, the poly-L-lysine (PLL), a cationic polymer rich in amino groups was used to electrostatically attach carboxylated CNT (COOH-CNT) in order to form a stable nanostructured film (COOH-CNT) with a high electroactive area. The nanohybrid compound of charged polymeric matrix on the electrode surface was obtained by electrodeposition techniques, providing functional groups to immobilize the carbohydrate-specific lectin. A label-free electrochemical biosensor developed to prostate tumor allowed to distinguish the glycoprotein profile in human serum.

2. Material and methods

2.1. Reagents

PLL, fetuin, bovine serum albumin (BSA), galactose and fucose were obtained from Sigma Aldrich (St. Louis, USA). Multi-walled carbon nanotubes functionalized with carboxylic groups (COOH-CNTs) (average diameter of ~ 10 nm, average length of 1–2 μm and 95% purity) were acquired from DropSens (Oviedo, ESP). *Cramoll* 1,4 (preparation containing isoforms 1 and 4 of *C. mollis* lectin) were obtained from the Protein Biochemistry Laboratory (UFPE) (Recife, BRA), according to protocol established by Correia and Coelho (1995). Fructose, glucose, glycine, dimethylformamide (DMF), potassium ferrocyanide ($K_4Fe(CN)_6$) and potassium ferricyanide ($K_3Fe(CN)_6$) were purchased from Vetek (São Paulo, BRA). The other reagents used were of analytical grade. The phosphate buffer saline (PBS) solution (0.01 mol L^{-1}, pH 7.4) was utilized in the experiments for sample dilution. The ultrapure water obtained from a water purification system Milli-Q (Billerica, USA) (18 MΩ) was utilized to prepare all solutions.

The serum samples were obtained from BPH and PCa patients that were confirmed via histopathological examination of prostate tissue. PCa patients were previously stratified by biopsy in the Gleason score of the 6, 7 and 9. All voluntary donors were admitted to the University Hospital of the UFPE (Recife, BRA), in accordance with the recommendations of the ethics committee. Venous blood samples were collected and immediately centrifuged at 1500 × *g* for 5 min The samples were stored at −20 °C while it is not in use.

2.2. Apparatus

The electrochemical studies were performed by using a potentiostat/galvanostat portable Ivium Compact Stat (Eindhoven, NLD) connected to a microcomputer and controlled by IviumSoft software. It was used a three electrode system, comprising a glassy carbon electrode (GCE) (Ø=3 mm) as the working electrode, a helical platinum wire as counter electrode and Ag/AgCl (KCl saturated) as the reference electrode.

The morphological characterization of the sensor surface was performed by the Scanning Electron Microscopy (SEM) technique by using a Philips XL-30 FEG microscope (Eindhoven, NDL). The measurements were recorded at acceleration voltage of 10 kV in low-vacuum mode and working distance of 1 μm. The structural characterization was accomplished with Fourier Transform Infrared in the Attenuated Total Reflectance mode (ATR FT-IR) using the Bruker IFS 66 model FT-IR spectrometer (Billerica, USA). Spectra were acquired at 4000 cm^{-1}–500 cm^{-1}, through a glassy carbon disc (~0.5 cm diameter) that was adapted to the electrochemical cell for further modifications.

2.3. Preparation of the nanoelectrode

Prior to modification, the GCE was polished with alumina powder (1 and 0.5 μm) for 3 min until obtaining a mirror-like surface. In order to remove any impurities, cleaned electrode was carefully rinsed with ultrapure water. After this step, the PLL (0.05 μmol L^{-1}) prepared in PBS solution (0.01 mol L^{-1}, pH 7.4) was electrochemically deposited on the GCE surface through the CV technique in the potential range −2.0 to 2.0 V at scan rate of 0.05 V s^{-1} for 15 cycles. Then, three layers of the COOH-CNT solution (15 μL) was deposited onto the GCE surface modified with PLL. The COOH-CNT solution consisted of 1 mg of COOH-CNT dispersed in 1 mL of DMF and sonicated in an ultrasonic bath for 2 h. Each layer was dried at 40 °C for evaporation of the solvent.

2.4. Immobilization of Cramoll 1,4 on the nanoelectrode

Cramoll 1,4 (200 μg mL^{-1}) was immobilized on the nanoelectrode during 60 min The working electrode was maintained in a moist chamber at room temperature (~ 25 °C). Finally, 5 μL of the glycine solution (0.05 mol L^{-1}), prepared in ultrapure water, was pipetted on the sensor surface for 60 min in order to blocking the nonspecific sites. The Fig. 1 shows the stepwise of the biosensor preparation.

2.5. Analytical response of the Cramoll 1,4 nanoelectrode

The analytical performance of the as-prepared nanoelectrode was evaluated through the incubation with 10 μL of fetuin at different concentrations. The samples diluted in PBS solution (0.01 mol L^{-1}, pH 7.4) were placed during 20 min in a moist chamber at room temperature. The analytical responses were monitored by SWV in a label-free assay by using $K_3Fe(CN)_6$/$K_4Fe(CN)_6$ (0.005 mol L^{-1}) as redox probe. The SWV analysis was carried out in a potential range of 0.0–0.4 V at frequency of 10.0 Hz.

The detection of lectin affinity was standardized by using the percentual decrease of current (ΔI%) in the SWV measurements

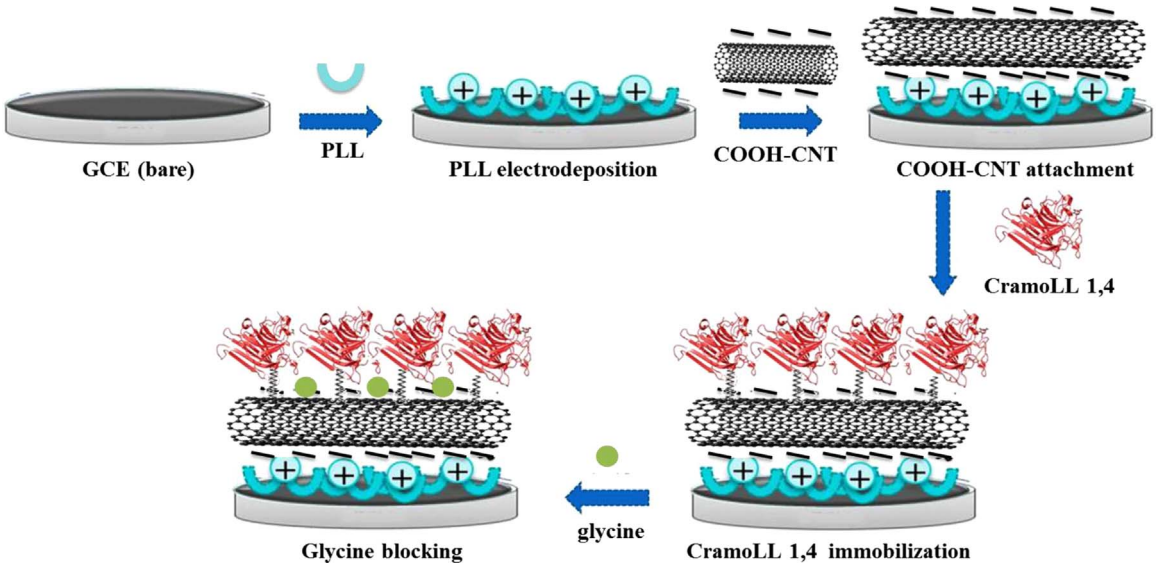

Fig. 1. Schematic illustration of the stepwise modification of the CramoLL 1,4 lectin nanoelectrode.

before and after carbohydrate incubation. A pool of serum of BPH and PCa patients diluted 1:30 in PBS solution (0.01 mol L^{-1}, pH 7.4) was used to evaluate the analytical responses. All measurements were carried out in triplicate.

The stepwise of the biosensor modifications were accomplished through CV measurements. The analysis was carried out in a potential range of −0.1 to 0.5 V, at 0.05 V s^{-1} scan rate, in presence of 0.005 mol $L^{-1}$of the $K_3Fe(CN)_6$/ $K_4Fe(CN)_6$ prepared in KCl solution (0.1 mol L^{-1}).

3. Results and discussion

3.1. Characterization of the nanoelectrode

In order to characterize the interaction of the COOH-CNTs with PLL as nanosurface support and the *Cramoll* 1,4 immobilization, comparative spectra of the modified GCE were evaluated by FT-IR analyses (Fig. 2**)**. PLL spectrum **(curve I)** exhibits two peaks at 3406 and 3271 cm^{-1} characteristic of the primary –NH_2 of the polymer. Another peak at 3063 cm^{-1} is attributed to the –NH_2^+ groups due to protonation of –NH_2 of PLL in PBS solution (0.01 mol L^{-1}, pH 7.4), taking account that pKa of polymer is found at 10.7 (Barth, 2007; Wang et al., 2012). The peaks at 1612 and 1525 cm^{-1} are ascribed to the amide I (C=O stretching vibration) and II (N–H bending vibration and C–N stretching vibration) bands

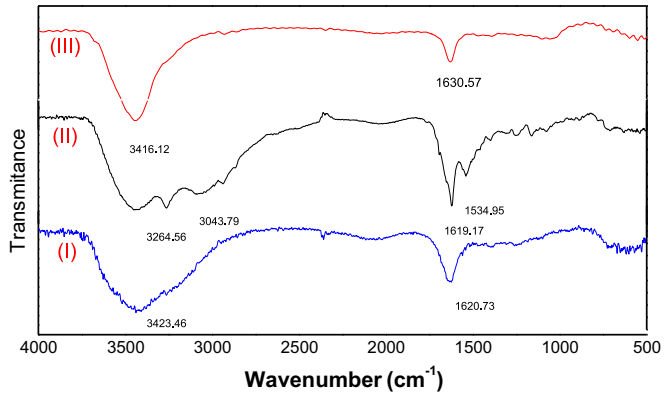

Fig. 2. FTIR spectra of the GCE modified with (I) COOH-CNT, (II) PLL and (III) COOH-CNT/PLL.

of the polypeptide PLL (Barth, 2007). The spectrum of COOH-CNT **(curve II)** shows a peak at 3320 cm^{-1} indicator of –OH groups; a peak at 1655 cm^{-1}, resulting from molecular elongation of C=O group, and another peak at 1002 cm^{-1} attributed to the C–O stretching vibration. These peaks are typically related to the carboxylic groups of the CNTs (Silva et al., 2014). The spectrum of COOH-CNT/PLL **(curve III)** exhibits a peak at 3335 cm^{-1} and other peaks at 1670 cm^{-1}, 1514 cm^{-1} and 1019 cm^{-1}, similar to COOH-CNT spectrum, confirming that nanotubes were anchored onto the PLL. Cationic polymers, such as PLL have been often used for the electrostatic interaction and ionic interaction between the positively charged polymer and COO^- groups of the CNT (Jiang et al., 2008; Fujigaya and Nakashima, 2015). Regarding the immobilization of *Cramoll* 1,4, the spectrum revealed two peaks at 3373 cm^{-1} and 3265 cm^{-1} attributed to primary -NH_2 and the peaks at 1621 cm^{-1} and 1521 cm^{-1} characteristic of the amide I (C=O stretching vibration) and II (N-H bending vibration and C-N stretching vibration) bands of *Cramoll* 1,4 and COOH-CNT interaction.

The stepwise modification of GCE surface was also characterized by SEM technique. Firstly, Fig. 3**a** shows GCE surface after electrodeposition of the PLL film with a thin layer of the polymer homogeneously distributed on the sensor surface. The micrograph of Fig. 3**b** exhibited an irregular surface formed by abundant spaghetti-like filamentous structures attributed to the COOH-CNT presence (Jiang et al., 2008). The deposition of carbon nanotubes on PLL/GCE surface showed a porous three-dimensional nanostructured film (Xue et al., 2011).

In order to evaluate the operational stability of COOH-CNT/PLL film, the modified GCE was submitted to 20 consecutive voltammetric cycles in $K_3Fe(CN)_6$/ $K_4Fe(CN)_6$ (0.005 mol L^{-1}). The relative standard deviation (RSD) estimated for current peak values of COOH-CNT/PLL was found at 0.6% showing a good stability of nanostructured film. To evaluate the role of PLL in assure to CNT binding, a control experiment was carried without PLL film. It was found a RSD of approximately 2.7% demonstrating that COOH-CNT/PLL was around four times more electrochemically stable than COOH-CNT straight on the electrode surface. This result can be ascribed to electrostatic interaction between cationic PLL and carboxylic groups of nanotubes (Jiang et al., 2008).

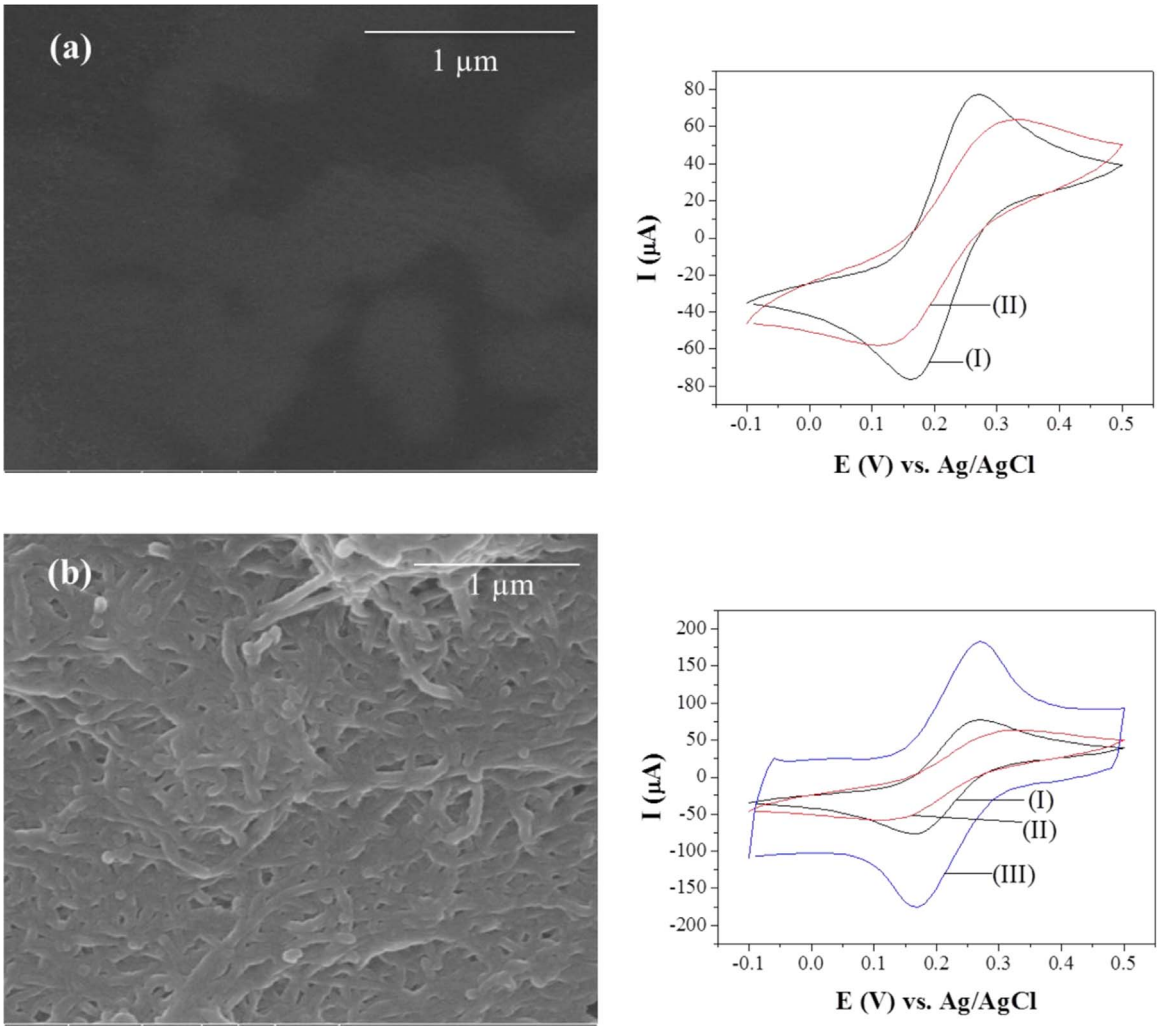

Fig. 3. SEM images and CVs of the surface (a) PLL/ GCE and (b) CNT/PLL/GCE. In a) and b), (I) GCE after cleaning; (II) PLL/GCE; (III) COOH-CNT/PLL/GCE. Measurements performed in $K_3Fe(CN)_6/K_4Fe(CN)_6$ (0.005 mol L^{-1}) prepared in KCl solution (0.1 mol L^{-1}).

3.2. Electrochemical characterization of lectin nanoelectrode

Fig. 4**a** shows the electrochemical characterization of construction steps of the biosensing platform. The monitoring of modifications from the electrode surface was performed by using CV technique in $K_3Fe(CN)_6$/ $K_4Fe(CN)_6$ as redox probe. The analysis of redox peaks of voltammograms after modification of GCE with PLL (0.05 μmol L^{-1}) (**curve II**) exhibits a reduction in the current amplitude when compared as the cleaned electrode (**curve I**). The electroactive area of GCE (0.096 cm^2), calculated according to Randles-Sevcik equation (Bard and Faulkner, 2001), showed a decrease after the PLL film (0.0079 cm^2). This result is attributed to the non-conducting nature of the polymer (Tsai et al., 2011), which confirms the electrodepositing of PLL on the sensor surface. After deposition of COOH-CNT on the PLL film (**curve III**), the voltammogram showed an increase in electroactive area (0.225 cm^2), that can be attributed to higher electron transfer promoted by the increase of conductivity due to COOH-CNTs (Zhu et al., 2012).

The immobilization of the *Cramoll* 1,4 onto COOH-CNT/PLL film is represented by a reduction in the amplitude of redox peaks in voltammograms (**curve IV**). The insulating nature of the biomolecule promotes a decreased of 11.5% of electroactive area from the electrode (0.202 cm^2). After blocking of the free reactive sites with glycine (**curve V**), it also was observed a slight reduction in charge transfer on the electrode surface.

The electron diffusion study of the COOH-CNT/PLL nanosurface with *Cramoll* 1,4 immobilized was investigated submitting the electrode to different scan rates. As can see in Fig. 4**b**, the voltammograms registered in a $K_3Fe(CN)_6/K_4Fe(CN)_6$ (0.005 mol L^{-1}) exhibit a proportional increase in both cathodic and anodic peak currents (I_{pa} and I_{pc}, respectively) according to the scan rate (10–120 mV s^{-1}). The I_{pa} and I_{pc} were directly proportional to the square root of scan rates (Fig. 4**b - *inset***) with the following linear regression equations: I_{pa} (μA) = $31.69*v^{1/2} - 57.27$ (r = 0.997) and I_{pc} (μA) = $-29.73*v^{1/2} + 50.23$ (r = 0.995). These results suggest that the reactions on the sensor interface were controlled by mass transport (surface diffusion), in agreement with the quasi-reversible system (Kang et al., 2009).

3.3. Experimental optimization

In order to achieve the optimal performance of the COOH-CNT/PLL film, the influence of PLL concentrations (0.0001 μmol L^{-1} to 0.2 μmol L^{-1}) was evaluated. In this study, a proportional increase in the amplitude of the peak currents in relation to PLL concentrations was found until reach a maximal response at 0.05 μmol L^{-1} of polymer (Fig. S1a **- Supplementary data**). Then, the COOH-CNTs concentrations (0.5 mg mL^{-1} to 3.5 mg mL^{-1}) deposited on the PLL film were investigated. The current peaks increased until the concentration of 1.5 mg mL^{-1} of nanotube (Fig. S1b **- Supplementary data**). After this point, the current decreased indicating a saturation of free reactive groups of polymer in the

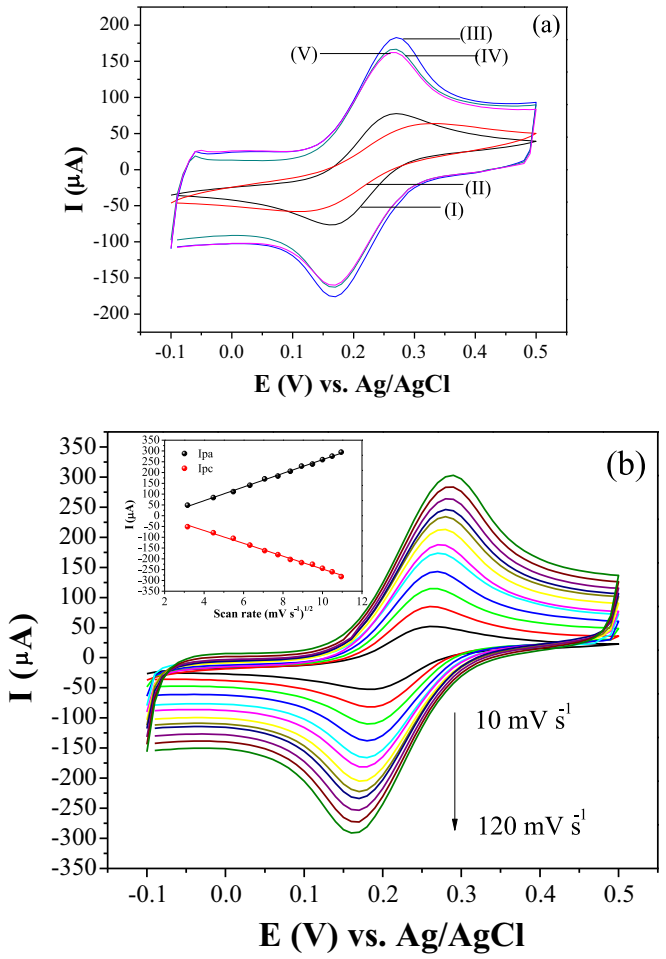

Fig. 4. **(a)** CVs of the stepwise modification of the lectin nanoelectrode: (I) GCE; (II) PLL/GCE; (III) COOH-CNT/PLL/GCE; (IV) CramoLL 1,4/COOH-CNT/PLL/GCE; (V) glycine/CramoLL 1,4/COOH-CNT/PLL/GCE; **(b)** Voltammetric profile of the CramoLL 1,4/COOH-CNT/PLL/GCE under different scan rates (10, 20, 30, 40, 50, 60, 70, 80, 90, 100, 110 and 120 mV s^{-1}) (*inset*: plots of the I_{pa} and I_{pc} *vs.* square roots of the scan rates). All the measurements were performed in $K_3Fe(CN)_6$/ $K_4Fe(CN)_6$ (0.005 mol L^{-1}) prepared in KCl solution (0.1 mol L^{-1}).

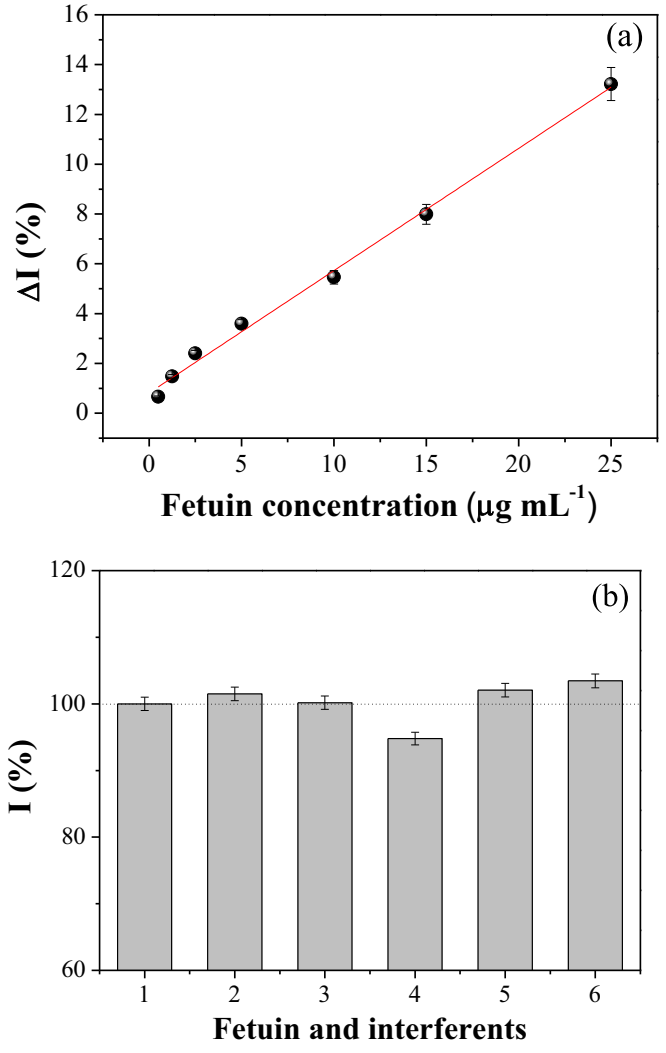

Fig. 5. **(a)** Analytical curve of the CramoLL 1,4 lectin nanoelectrode for different fetuin concentrations (0.5–25 μg mL^{-1}) obtained by SWV measurements in $K_3Fe(CN)_6$/ $K_4Fe(CN)_6$ (0.005 mol L^{-1}) prepared in KCl (0.1 mol L^{-1}); **(b)** Electrochemical response of the CramoLL 1,4 lectin nanoelectrode for interferents molecules: (1) fetuin (25 μg mL^{-1}); (2) glucose (500 μg mL^{-1}); (3) galactose (500 μg mL^{-1}); (4) fructose (500 μg mL^{-1}); (5) fucose (500 μg mL^{-1}) and (6) and BSA (5 g L^{-1}).

sensor surface.

The amount of the *Cramoll* 1,4 immobilized on the COOH-CNT/PLL film is a limiting aspect in the biosensing platform to obtain a good analytical sensitivity. Thus, the different concentrations (1–200 μg mL^{-1}) of *Cramoll* 1,4 immobilized on the nanosurface were evaluated (Fig. S1c - **Supplementary data**). The electrode response showed a proportional increase of current value in relation to *Cramoll* 1,4 concentrations with a maximal lectin-nanosurface interaction at 200 μg mL^{-1}.

3.4. Analytical response of the lectin sensor to fetuin

The activity of *Cramoll* 1,4 was analysed through the correlation of the electrochemical measurements at different glycans concentrations. In this study, fetuin was chosen to evaluate the carbohydrate specific of *Cramoll* 1,4. Different electrodes were incubated with 10 μL of fetuin solutions at specific concentrations during 20 min Then, the electrodes were submitted to SWV measurements in $K_3Fe(CN)_6/K_4Fe(CN)_6$ solution (0.005 mol L^{-1}) prepared in KCl (0.1 mol L^{-1}). The label-free SWV detection is based on interfacial resistance to electron transfer of the $K_3Fe(CN)_6/K_4Fe(CN)_6$ probe after successive incubations of the sensor surface with fetuin solution. The results were examined in terms of relative current variation (ΔI%) according to the following equation: $\Delta I\% = [I_{(Cramoll\ 1,4)} - I_{(Cramoll\ 1,4\text{-glycoprotein})}/I_{(Cramoll\ 1,4)}] \times 100$, where $I_{(Cramoll\ 1,4)}$ is the current value of the biosensor as-prepared and $I_{(Cramoll\ 1,4\text{- glycoprotein})}$ is the current value after exposure to glycoprotein. The analytical responses of the biosensor showed a linear enhance in the ΔI% with the augment of fetuin concentrations (Fig. 5**a**). The curve revealed the following linear regression equation: $\Delta I_{(fetuin)} = 0.49*[fetuin] + 0.81$ ($r = 0.994$, $p < 0.001$, $n = 7$). The analytical sensibility of the nanoelectrode for fetuin was of 2460 μA M^{-1} cm^{-2}. The major analytical sensibility to fetuin confirms the greater affinity of the *Cramoll* 1,4 in detection of the glycoproteins for characterization of serum glycoproteins (Lima et al., 1997; Oliveira et al., 2008). The limit of detection (LOD) was statically determinate as: $3.3RSD_{blank}/b$, where RSD_{blank} is the RSD of the blank and b is the slope calculated of the analytical curve. The LOD achieved by nanoelectrode for fetuin was 0.017 μg mL^{-1} that was found higher than lower LOD described biosensor for fetuin glycoprotein (Bertok et al., 2013; Kluková et al., 2014), although this biosensor has used the SNA I lectin from *Sambucus nigra*. On the other hand, fetuin biosensors with similar or lower LOD described require impedimetric responses

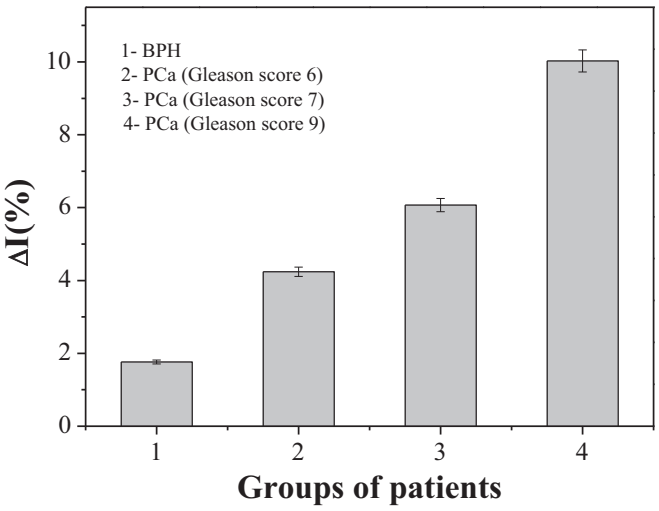

Fig. 6. Electrochemical response of the CramoLL 1,4 lectin nanoelectrode for serum samples of patients with (1) BPH, (2) PCa (Gleason score 6), (3) PCa (Gleason score 7) and (4) PCa (Gleason score 9). Measurements obtained by SWV assays performed in $K_3Fe(CN)_6/K_4Fe(CN)_6$ (0.005 mol L^{-1}) solution prepared in KCl (0.1 mol L^{-1}).

(Oliveira et al., 2011), which involve more sophisticated and complicated analyses than SWV techniques.

3.5. Reproducibility, repeatability, long-term stability and interference study

The reproducibility and repeatability are crucial parameters to evaluate the operational performance of the biosensor. The reproducibility was estimated through the response of 8 different electrodes incubated with fetuin (5 μg mL^{-1}) under optimal conditions. The nanoelectrodes showed an acceptable RSD of 4.24% (< 5%). The repeatability of the nanoelectrode, pre-incubated with fetuin (5 μg mL^{-1}), was obtained through 20 successive measurements with an interval of 1 min The nanoelectrode exhibited an excellent repeatability with an RSD of 1.24% (< 5%).

The long-term stability of the lectin nanoelectrode was tested using six electrodes. The electrodes were incubated with a solution of fetuin (5 μg mL^{-1}) under optimal conditions in the intervals of 1, 3, 5, 7 and 15 days. The nanoelectrode during the study was maintained in a moist chamber at 4 °C. The SWV responses revealed a good stability showing that 79.55% of the analytical response was preserved after 15 days.

Prior to application in assays with serum samples, an interference study was performed by addition of pattern with several species in order to investigate the specificity of the biosensor. The nanoelectrodes were incubated with 10 μL of solution contenting only fetuin (25 μg mL^{-1}), as control, and a fetuin solution (25 μg mL^{-1}) plus interferents. Five interferents were selected and among these BSA, an abundant protein present in serum sample, and monosaccharides which can be found in bloodstream and glycoproteins. The interferents on the solutions were found at final concentrations: 500 μg mL^{-1} glucose, 500 μg mL^{-1} galactose, 500 μg mL^{-1} fructose, 500 μg mL^{-1} fucose and 5 g L^{-1} BSA. The degree of interference was determined considering the response of current for control sample as 100%. Calculated recoveries were 105.1 ± 1.01% for glucose, 100.18 ± 1.00% for galactose, 94.8 ± 0.95% for fructose, 102.06 ± 1.02% for fucose and 103.45 ± 1.03% for BSA (Fig. 5**b**), with average value of 101.12 ± 1.00%. The results obtained revealed a low degree of interference (less than 10%) on nanoelectrode response, being higher for fructose.

3.6. Glycoprofiling detection in serum samples with lectin nanoelectrode

The proposed lectin nanoelectrode was applied to detection of glycoproteins in sera of patients with BPH and PCa confirmed via histopathological examination. The *Cramoll* 1,4 nanoelectrode was incubated with pools of serum samples diluted 1:30 in PBS and then submitted to SWV analysis in 0.005 mol L^{-1} $K_3Fe(CN)_6/K_4Fe(CN)_6$ prepared in 0.1 mol L^{-1} KCl. The results in Fig. 6 show that the *Cramoll* 1,4 nanoelectrode was able to screen glycosylation profiles of patients with BPH and PCa. The analytical response exhibited a proportional increase in ΔI% value for PCa samples with Gleason score of 6, 7 and 9. The increase in electrochemical response was statistically significant for all observed samples according to ANOVA test ($p < 0.02$). The dates analysed by Student *t*-test, at a 95% confidence level, show highly significant difference between all PCa samples (scores 6, 7 and 9) and BPH sample ($p < 0.01$).

Quantitative alterations of glycoproteins in sera of PCa patients analysed by mass spectrometry have demonstrated that glycan levels tend to rise with the Gleason score and predict the prognosis of cancer (Drake et al., 2006; Saldova et al., 2011). Patients with PCa Gleason scores 7 or higher to this have increased risk of metastasis and recurrence after therapy (Pierorazio et al., 2013). This proposed nanoelectrode showed an excellent performance and is the first report using *Cramoll* lectin to distinguish benign hyperplasia and Gleason scores in serum samples. However, studies that are more detailed associated with immunoassay in human serum for PCa diagnostic concentrations are necessary to indicate this system as an alternative approach to apply in clinical routine.

4. Conclusions

Cramoll 1,4 lectin nanoelectrode based on COOH-CNT and PLL showed to be sensitive to differentiate serum glycoprotein profiles of patients with BPH and PCa advanced Gleason score, providing a potential tool for PCa staging. However, additional studies with a higher number of samples and correlation with other techniques are required to validate these important finding, taking account that PCa is a multifactorial disease.

Acknowledgements

The authors are grateful for the assistance provided by the Pernambuco State Foundation for the Support of Science and Technology (FACEPE), National Council of Technological and Scientific Development (CNPq) and CNPq for fellowships.

Appendix A. Supplementary material

Supplementary data associated with this article can be found in the online version at http://dx.doi.org/10.1016/j.bios.2016.05.004.

References

Ahmed, M.U., Hossain, M.M., Safavieh, M., Wong, Y.L., Rahman, I.A., Zourob, M., Tamiya, E., 2016. Crit. Rev. Biotechnol. 36 (3), 495–505.
Bard, A.J., Faulkner, L.R., 2001. Electrochemical Methods: Fundamentals and Applications, 2nd ed. Wiley, New York (2001).
Barth, A., 2007. BBA 1767, 1073–1101.
Bertok, T., Gemeiner, P., Mikula, M., Gemeiner, P., Tkac, J., 2013. Microchim. Acta 180, 151–159.

Correia, M.T.S., Coelho, L.C.B.B., 1995. Appl. Biochem. Biotechnol. 55, 261–273.
Drake, R.R., Schwegler, E.E., Malik, G., Diaz, J., Block, T., Mehta, A., Semmes, O.J., 2006. Mol. Cell. Proteom. 5 (10), 1957–1967.
Freitas, T.A., Mattos, A.B., Silva, B.V.M., Dutra, R.F., 2014. Biomed. Res. Int. 2014 (13), 929786.
Fujigaya, T., Nakashima, N., 2015. Sci. Tech. Adv. Mater. 16, 24802–24823.
Gomes-Filho, S.L.R., Dias, A.C.M.S., Silva, M.M.S., Silva, B.V.M., Dutra, R.F., 2013. Microchem. J. 109, 10–15.
Heidenreich, A., Bastian, P.J., Bellmunt, J., Bolla, M., Joniau, S., van der Kwast, T., Mason, M., Matveev, V., Wiegel, T., Zattoni, F., Mottet, N., 2014. Eur. Urol. 65, 124–137.
Jiang, C., Yang, T., Jiao, K., Gao, H., 2008. Electrochim. Acta 53, 2917–2924.
Kang, X., Wang, J., Wu, H., Aksay, I.A., Liu, J., Lin, Y., 2009. Biosens. Bioelectron. 25, 901–905.
Kluková, L., Bertok, T., Kasák, P., Tkac, J., 2014. Anal. Methods 6, 4922–4931.
La Belle, J.T., Gerlach, J.Q., Svarovsky, S., Joshi, L., 2007. Anal. Chem. 79 (18), 6959–6964.
Lima, V.L.M., Correia, M.T.S., Cechinel, Y.M.N., Sampaio, C.A.M., Owen, J.S., Coelho, L. C.B.B., 1997. Carbohydr. Polym. 33, 27–32.
Liu, X., Duckworth, P.A., Wong, D.K.Y., 2010. Biosens. Bioelectron. 25, 1467–1473.
Ma, P., Siddiqui, N.A., Marom, G., Kim, J., 2010. Compos. Part A 41, 1345–1367.
Mintz, P.J., Rietz, A.C., Cardó-Vila, M., Ozawa, M.G., Dondossola, E., Do, K., Kim, J., Troncoso, P., Logothetis, C.J., Sidman, R.L., Pasqualini, R., Arap, W., 2015. Proc. Natl. Acad. Sci. USA 112 (8) 2515–2120.
Moyer, V.A., 2012. Ann. Intern. Med. 157 (2), 120–135.
Oliveira, M.D.L., Correia, M.T.S., Coelho, L.C.B.B., Diniz, F.B., 2008. Colloids Surf. B: Biointerfaces 66, 13–19.
Oliveira, M.D.L., Nogueira, M.L., Correia, M.T.S., Coelho, L.C.B.B., Andrade, C.A.S., 2011. Sens. Actuators B – Chem. 155, 789–795.
Pierorazio, P.M., Walsh, P.C., Partin, A.W., Epstein, J.I., 2013. BJU Int. 111, 753–760.
Rho, J., Roehrl, M.H.A., Wang, J.Y., 2009. Protein J. 28, 148–160.
Sakwe, A.M., Koumangoye, R., Goodwin, S.J., Ochieng, J., 2010. J. Biol. Chem. 285 (53), 41827–41835.
Saldova, R., Fan, Y., Fitzpatrick, J.M., Watson, R.W.G., Rudd, P.M., 2011. Glycobiology 21 (2), 195–205.
Schover, L.R., Fouladi, R.T., Warneke, C.L., Neese, L., Klein, E.A., Zippe, C., Kupelian, P. A., 2002. Cancer 95 (11), 2397–2407.
Siegel, R., Ma, J., Zou, Z., Jemal, A., 2014. CA Cancer J. Clin. 14 (64), 9–29.
Silva, M.M.S., Dias, A.C.M.S., Silva, B.V.M., Gomes-Filho, S.L.R., Kubota, L.T., Goulart, M.O.F., Dutra, R.F., 2014. J. Chem. Technol. Biotechnol. 90 (1), 194–200.
Tsai, T., Wang, S., Chen, S., 2011. Electroanal. Chem. 659, 69–75.
Vashist, S.K., 2012. Diagnostics 2, 23–33.
Vashist, S.K., Schneider, E.M., Luong, J.H.T., 2014. Analyst 139, 2237–2242.
Vashist, S.K., Schneider, E.M., Luong, J.H.T., 2015a. Biosens. Bioelectron. 67, 73–78.
Vashist, S.K., Schneider, E.M., Luong, J.H.T., 2015b. Anal. Chim. Acta 883, 74–80.
Wang, F., Jiang, F., Li, Y., Wang, Q., Zhang, X., 2012. RSC Adv. 2, 5738–5747.
Xue, Y., Bao, L., Xiao, X., Ding, L., Lei, J., Ju, H., 2011. Anal. Biochem. 410, 92–97.
Yi, J.K., Chang, J.W., Han, W., Lee, J.W., Ko, E., Kim, D.H., Bae, J., Yu, J., Lee, C., Yu, M., Noh, D., 2009. Cancer Epidemiol. Biomark. Prev. 18 (5), 1357–1364.
Zhu, Z., Garcia-Gancedo, L., Flewitt, A.J., Xie, H., Moussy, F., Milne, W.I., 2012. Sensors 12, 5996–6022.